NANO LETTERS

2009
Vol. 9, No. 5
2054-2058

Hybrid Core−Shell Nanowire Forests as Self-Selective Chemical Connectors

Hyunhyub Ko,[†,‡,§,||] Jongho Lee,[†,⊥] Bryan E. Schubert,[†,‡] Yu-Lun Chueh,[‡,§,||] Paul W. Leu,[‡,§,||] Ronald S. Fearing,[*,‡] and Ali Javey[*,‡,§,||]

Department of Electrical Engineering and Computer Sciences, University of California at Berkeley, Berkeley, California 94720, Materials Sciences Division, Lawrence Berkeley National Laboratory, Berkeley, California 94720, Berkeley Sensor and Actuator Center, University of California at Berkeley, Berkeley, California 94720, and Department of Mechanical Engineering, University of California at Berkeley, Berkeley, California 94720

Received February 2, 2009; Revised Manuscript Received March 15, 2009

ABSTRACT

Conventional connectors utilize mechanical, magnetic, or electrostatic interactions to enable highly specific and reversible binding of the components (i.e., mates) for a wide range of applications. As the connectors are miniaturized to small scales, a number of shortcomings, including low binding strength, high engagement/disengagement energies, difficulties with the engagement, fabrication challenges, and the lack of reliability are presented that limit their successful operation. Here, we report unisex, *chemical* connectors based on hybrid, inorganic/organic nanowire (NW) forests that utilize weak van der Waals bonding that is amplified by the high aspect ratio geometric configuration of the NWs to enable highly specific and versatile binding of the components. Uniquely, NW *chemical* connectors exhibit high macroscopic shear adhesion strength (∼163 N/cm^2) with minimal binding to non-self-similar surfaces, anisotropic adhesion behavior (shear to normal strength ratio ∼25), reusability (∼27 attach/detach cycles), and efficient binding for both micro- and macroscale dimensions.

At millimeter dimensions or less, the conventional mechanical, electrostatic, and magnetic connectors[1,2] suffer from severe performance and reliability degradation that presents a major challenge for applications that require specific binding of miniaturized components.[3,4] Therefore, there is a major need for a new connector concept that perhaps operates with a different binding principle. In contrast to the conventional connectors (e.g., buttons, zippers, and Velcro), universal adhesives (e.g., tapes, glues, and synthetic gecko adhesives)[5−10] enable efficient binding even for miniaturized components as they utilize chemical binding interactions which maintain their binding ability with size reduction. A challenge in using chemical binding interactions[11−14] for connector applications arises in the need for reversible *and* specific, rather than permanent and universal binding between the components. For instance, while van der Waals (vdW) interactions are reversible, they are highly nonspecific which enables the gecko adhesives to bind efficiently to various surfaces with ease[5−11]—a nonideal property for connectors. To address the need for a new connector technology, here we report *chemical* connectors that utilize reversible vdW bonding interactions of hybrid inorganic/organic NW forests. The weak vdW bond strengths result in the low adhesion of the relatively stiff, hybrid NWs on non-self-similar surfaces, in distinct contrast to nanotube or polymeric-based synthetic gecko adhesive which utilize materials with lower stiffness. However, high shear adhesion is obtained once the hybrid NW forests are engaged with self-similar surfaces due to the drastic amplification of the contact area arising from the interpenetration of the high-aspect ratio NWs. As a result, highly specific and versatile *chemical* connectors with unique properties are enabled that exhibit tunable properties through composition control of the hybrid NW components.

In this study, Ge NW forests (diameter, $d = 20-30$ nm and length, $L \sim 30$ μm) were utilized as the backbone of the *chemical* connectors (Figure 1a) to enable nanofibrillar structures with high aspect ratios (see Methods). Cross-sectional and top-view scanning electron microscopy (SEM) images (Figure 1b,c) of the Ge NW arrays indicate that most of the NWs are grown vertically on the substrate but with random orientation, resembling a forest. Clearly, the grown NWs sustain their high aspect ratio without aggregation or collapse (Figure 1b,c), in part due to the high Young's

* Corresponding authors: ajavey@eecs.berkeley.edu, ronf@eecs.berkeley.edu.
† These authors contributed equally.
‡ Department of Electrical Engineering and Computer Sciences, University of California at Berkeley.
§ Materials Sciences Division, Lawrence Berkeley National Laboratory.
|| Berkeley Sensor and Actuator Center, University of California at Berkeley.
⊥ Department of Mechanical Engineering, University of California at Berkeley.

10.1021/nl900343b CCC: $40.75 © 2009 American Chemical Society
Published on Web 04/24/2009

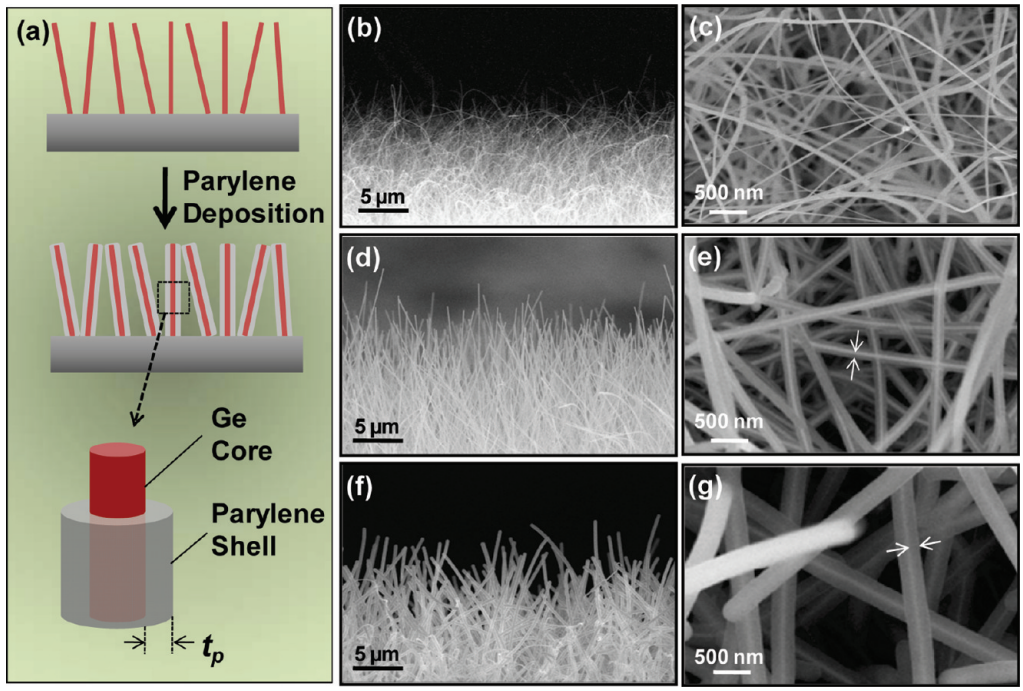

Figure 1. Ge/parylene core/shell hybrid NW forests for unisex, *chemical* connectors. (a) Schematic of the fabrication procedure for the core−shell NW forests. Cross sectional and top-view SEM images of Ge NWs (b, c) without parylene coating, (d, e) with 50 nm parylene coating, and (f, g) with 200 nm parylene coating, respectively. The white arrows in (e, g) indicate the parylene shell.

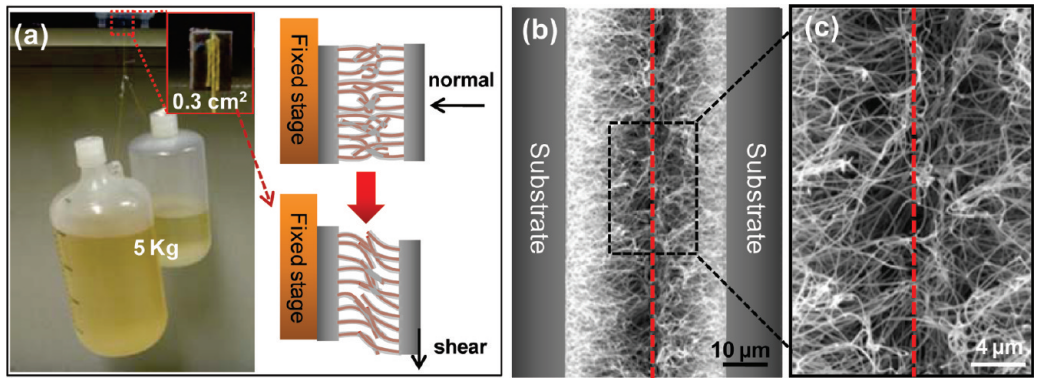

Figure 2. NW connectors in the engaged mode. (a) 5 kg of weight is suspended from a vertical surface by the use of NW connectors with a ∼30 mm^2 area. The schematic shows the interpenetrated NWs under a normal (top) and shear force (bottom). (b, c) Cross-sectional SEM images of the engaged NW connectors.

modulus (∼100−150 GPa)[15] of the Ge NWs. Next, a thin parylene layer with a thickness t_p = 10−400 nm was deposited in the gas phase, resulting in free-standing Ge/parylene core/shell NW arrays (Figure 1). The parylene coating was highly uniform (Figure 1) with minimal NW surface roughness as evident from transmission electron microscopy (TEM) analyses (see Figure S1 in Supporting Information). The parylene shell has three important functions. First, the compliance of the polymeric shells provides an intimate contact with the opposite surface, therefore increasing the vdW interactions in the engaged mode.[16] Second, the viscoelastic property of parylene prevents the brittle failure of NW arrays[17] and thus reinforces the mechanical robustness and reusability of the NW connectors. Finally, parylene is an ideal passivation material with superb chemical properties, including low permeability to most gases and water vapor, high chemical resistivity, and hydrophobic surface properties.[18]

The performance of the NW connectors was evaluated by macroscopic shear adhesion tests (Figure 2). An example of the strong binding achieved is shown in Figure 2a in which a hand-engaged NW connector with a surface area of ∼0.5 × 0.6 cm^2 enables 5 kg (∼49 N) of weight to be hung from a vertical surface without failure. This adhesion ability corresponds to a shear adhesion strength of ∼163 N/cm^2, well above the shear adhesion strengths obtainable by most connector technologies (Velcro 5−15 N/cm^2)[19] and comparable or better than those achieved with universal adhesives (carbon nanotube gecko adhesives ∼100 N/cm^2).[20] The strong shear binding arises from the large contact area between the interpenetrating NWs, effectively amplifying the vdW interactions.

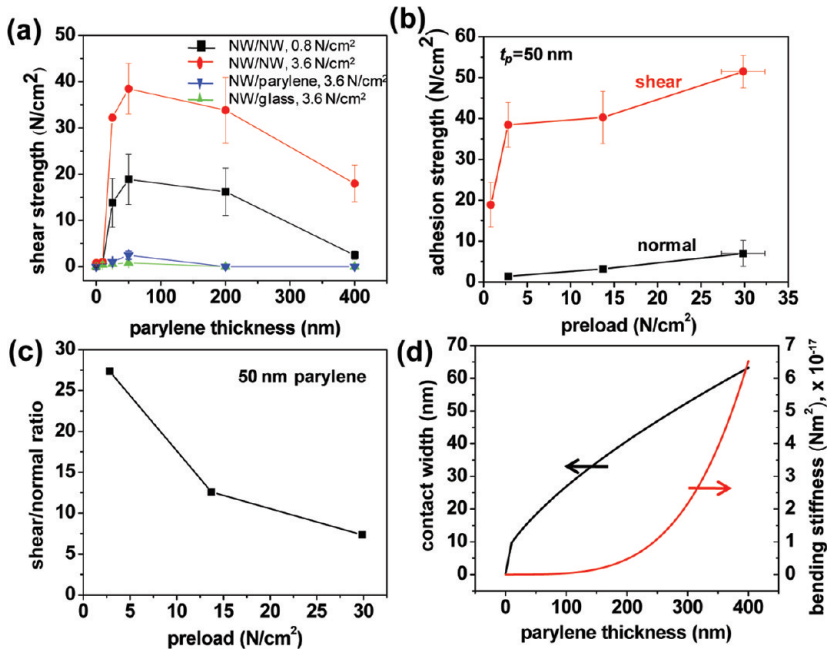

Figure 3. Adhesion characteristics of the NW connectors. (a) Shear strength of NW connectors as a function of the parylene shell thickness for normal preload forces of 0.8 and 3.6 N/cm^2. For comparison purposes, the shear strength of NW forests on glass (green curve) and parylene coated glass (blue curve) surfaces is also shown. (b) Shear and normal strength for $t_p = 50$ nm as a function of the normal preload. (c) Shear to normal strength ratio as a function of the preload, showing the anisotropic adhesion behavior of NW connectors. (d) The calculated contact width between two NWs overlapped by 5 μm under a normal force of 200 nN (black curve) and the bending stiffness of a single NW (red curve) as a function of the parylene shell thickness.

To further characterize the properties of NW connectors and shed light on their binding mechanism, we systematically measured the macroscopic shear adhesion strength as a function of the parylene shell thickness (Figure 3a). The measurements were conducted by first engaging the connectors (area ~0.3 cm^2) with a normal preload force. The preload force was then removed while a continuously increasing shear force was applied until a failure (i.e., detachment) was observed. The force at failure corresponds to the maximum shear strength of the connectors. As depicted in Figure 3a, the shear adhesion properties strongly depend on the thickness of the polymeric shell and the applied preload force. Specifically, a weak shear strength of ~0.8 N/cm^2 is attained for the pristine GeNWs (i.e., without a parylene shell) with a preload of ~3.6 N/cm^2. The shear strength, however, is drastically enhanced by the application of the parylene shell, with a maximum shear strength of ~38 N/cm^2 obtained for $t_p = 50$ nm and a preload of ~3.6 N/cm^2. This significant enhancement in the shear adhesion is attributed to the higher surface compliance of the parylene shell on the hard Ge NWs, enabling conformal contact with increased contact area between the interpenetrating NWs. This effect is clearly evident from the contact area calculations[21] between two parallel NWs based on the Hertz contact[22] for hard, pristine Ge NWs and Johnson−Kendall−Roberts mechanics[23] for parylene-coated Ge NWs, indicating a contact width enhancement of ~115× for $t_p = 50$ nm as compared to the pristine Ge NWs (Figure 3d, see Supporting Information for detailed calculations).

A decrease in the shear adhesion of NW connectors is observed for $t_p > 50$ nm. This trend is attributed to the higher stiffness for thicker parylene shells, which reduces the conformal side contact between the interpenetrating NWs. Specifically, the $t_p = 400$ nm NWs are calculated to have a bending stiffness ~1500 times that of the $t_p = 50$ nm NWs (Figure 3d). Additionally, the filling factor is increased for thicker parylene shells, which further reduces the NW interpenetration and the effective contact area. This hypothesis is directly confirmed by the microscale indentation tests, in which indentation depths of ~26 and 11 μm are observed for $t_p = 50$ and 200 nm, respectively (see Figure S2 in Supporting Information). To examine the effect of miniaturization on the binding properties of the NW chemical connectors, microscopic shear adhesion tests were performed. Similar binding properties were observed for microscopic tests (area = 1−5 mm^2), further confirming the generic characteristics of the NW connectors, independent of the connector size (see Figure S3 in Supporting Information). It should be noted that besides the shell thickness, the interpenetration depth of the NW connectors is expected to also depend on the NW length, especially since longer NWs tend to bend and collapse more readily. In the future, detailed studies of the geometric effects of the NW forests on the binding characteristics are needed to further optimize the connectors.

NW chemical connectors are highly nonsticky to foreign surfaces. As depicted in Figure 3a, the shear adhesion of NW connectors is strong for self-similar surfaces (i.e., surfaces with comparable geometric configuration to enable NW interpenetration) but weak on flat surfaces. For instance, NW forests with $t_p = 200$ and 400 nm, exhibit minimal (<0.8 N/cm^2) shear or normal adhesion on flat surfaces (i.e., glass

and parylene coated glass). This *self-selective* adhesion property arises from the drastically enhanced contact area (>25 times enhancement, see Supporting Information for detailed calculations) and intimate contact for the interpenetrating NW configuration as compared to that of NWs on flat surfaces (see Figure S2b in Supporting Information). This is highly attractive for connector applications where specific binding of the two components are desired, for instance, for reconfigurable structures (see Figure S4 in Supporting Information for a proof of concept demonstration), and presents a major contrast to the gecko adhesives which are highly sticky to most surfaces. As compared to the widely explored gecko-inspired adhesives which utilize carbon nanotube or polymeric fibrillar structures, the NW connectors have higher stiffness, especially for thick parylene shells, which reduces their contact area on flat surfaces.

Besides the parylene shell thickness, the shear adhesion strength is also affected by the preload force applied to engage the connectors. In general, a monotonic increase in the adhesion force is observed with the preload force (Figure 3b). Specifically, when the preload force is increased from 0.8 to 3.6 N/cm^2, an enhancement of ~2 times in the shear adhesion strength is observed for t_p = 50 nm, with the sensitivity of the adhesion strength decreasing for higher preloads (Figure 3b), and eventually reaching ~163 N/cm^2 for hand-engaged (preload ~100 N/cm^2) binding tests (Figure 2a). This behavior is expected since the higher preload force results in an enhanced contact area between the NWs by increasing the extent of the interpenetration. It is also worth noting that an adhesion coefficient (shear to preload ratio) of ~24 is obtained for a preload force of 0.8 N/cm^2 (Figure 3a), which is significantly higher than most gecko-inspired adhesives.[8,9,20,24,25] Since the adhesion coefficient represents the efficiency of binding with respect to the applied force, NW connectors are highly useful for assembly processes requiring minimal engagement energy between the components.

As depicted in Figure 3b,c, NW connectors exhibit significantly higher shear than normal strength, which is a desirable property for connector applications requiring reusability with easy detachment. Specifically, shear to normal adhesion ratios of ~27 and 7 are obtained for a preload force of 2.8 and 30 N/cm^2, respectively. This anisotropic adhesion behavior is due to the enhanced side contact between the interpenetrating NWs under a shear force. A shear force induces NW alignment in the shear direction (Figure 2a and see Figure S5 in Supporting Information), providing a higher probability of side contact between parallel NWs. Depending on the applied preload force (i.e., interpenetration depth), there seems to be two different shear failure modes, that is, interfacial and cohesive failure (see Figure S6 in Supporting Information). When the interpenetration depth is small, the interfacial vdW interaction is the limiting factor in determining the adhesion strength. However, beyond a critical interpenetration depth, the interfacial vdW interactions are strong enough to induce polymer necking and rupture of the hybrid NWs (see Figure S7 in Supporting Information), resulting in cohesive failure. Interestingly, within the interfacial failure mode, NW connectors show reusability up to 27 times for an applied shear force of 1.2 N/cm^2 and a preload force of 0.8 N/cm^2 (see Figure S8 in Supporting Information). This reusability may be further enhanced in the future through materials optimization.

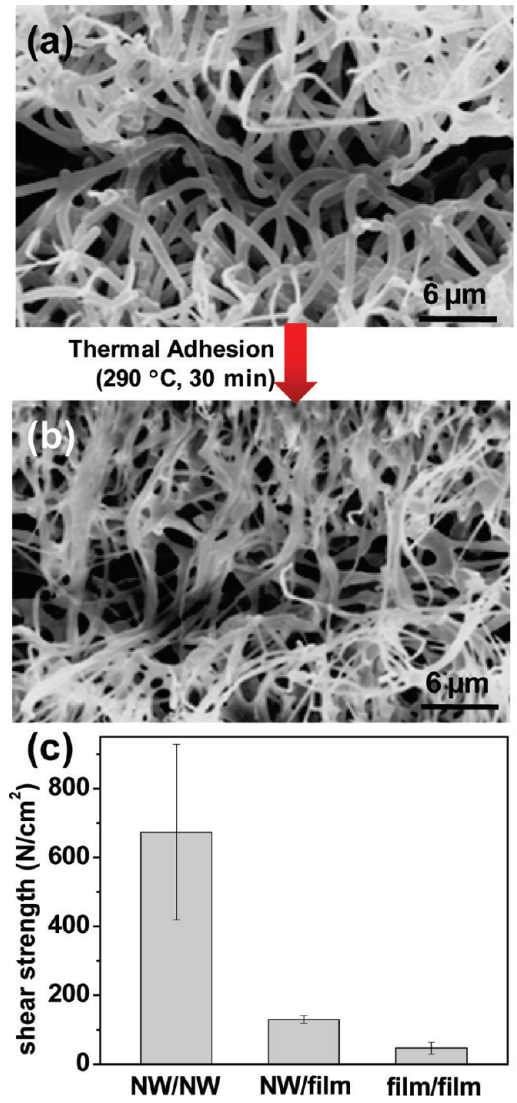

Figure 4. Permanent, thermal adhesion of NW connectors. Cross-sectional SEM images of interpenetrating NWs (a) before and (b) after the thermal adhesion at 290 °C for 30 min. (c) Comparison of the shear adhesion strength for NW/NW, NW/parylene film, and parylene film/parylene film after thermal adhesion at 290 °C for 30 min.

Besides vdW interactions, mechanical interlocking of the NWs, similar to those used in the hook and loop fasteners, may also affect the adhesion properties. In fact, the mechanical entanglement is evident from SEM images of the engaged NW connectors (Figure 2b,c). However, since the shear strength is significantly higher than the normal strength, we speculate that the mechanical interactions are not the dominant binding mechanism as such interactions are typically isotropic. Additionally, we find that when the surface of Ge/parylene NWs is hardened with enhanced surface roughness, for instance by depositing an ultrathin layer of Ti/Au (2/3 nm), a drastic decrease in the shear strength is

observed (see Figure S9 in Supporting Information). This result is indicative of the dominant role of the vdW interactions in NW connectors for which an intimate contact is essential.

Another unique feature of the hybrid NW connectors is their ability to controllably operate in either a reusable or permanent binding mode. The permanent binding mode is achieved through a thermal treatment of the engaged connectors during which the organic shell is melted, resulting in the bonding of the interpenetrating inorganic NWs from the two components (Figure 4a,b). The average observed shear strength of NW connectors after thermal adhesion at 290 °C (melting temperature of parylene-C used as organic shell) for 30 min is ~670 N/cm^2 with a maximum value of ~980 N/cm^2. This impressive shear adhesion strength is comparable to that of most instant adhesives (414−2000 N/cm^2, 3 M Scotch-Weld instant adhesives)[26] which shows the versatility of the hybrid NW forests as tunable connectors. Notably, the thermal adhesion for the interpenetrating NW connectors is well above the thermal adhesions obtained for planar parylene films (~50 N/cm^2) as depicted in Figure 4c, demonstrating the importance of the fibrillar geometry and inorganic components of the interpenetrating NWs in gaining high permanent binding strength.

In conclusion, highly versatile *chemical* connectors that utilize nanoscale surface chemical binding interactions are reported and characterized in depth. The connectors are unisex and consist of interpenetrating, inorganic/organic core/shell NW forests with the inorganic core serving as the backbone and the organic shell providing the strength and the surface compliance needed to enable large contact areas. Because of the weak vdW bond strengths, the relatively stiff hybrid NW forests are highly nonsticky to nonsimilar foreign surfaces. However, the vdW interactions are drastically amplified when the high aspect ratio NW forests are engaged with self-similar surfaces, resulting in large contact area between the interpenetrating NW components, with the maximum shear strength approaching ~163 N/cm^2. The NW stiffness and surface compliance are directly tuned by the thickness of the parylene shell, therefore enabling a high degree of control for both the specific binding and the shear strength.

Acknowledgment. We thank J. C. Ho and Z. Zhang for useful discussions and technical help. This work was supported by DARPA/DSO, NSF, and Berkeley Sensor and Actuator Center. The nanowire synthesis part of this project was supported by a Laboratory Directed Research and Development grant from Lawrence Berkeley National Laboratory.

Supporting Information Available: Descriptions of the nanowire growth, parylene coating, and macroscopic and microscopic adhesion tests, calculations of contact area and bending stiffness, and additional figures showing images of NWs and hybrid NWs, indentation tests, connector characterization, modeled shear strength, and resuability tests. This material is available free of charge via the Internet at http://pubs.acs.org.

References

(1) Yim, M.; Zhang, Y.; Roufas, K.; Duff, D.; Eldershaw, C. *IEEE/ASME Trans. Mechatron.* **2002**, *7*, 442.
(2) Cohn, M. B.; Böhringer, K. F.; Noworolski, J. M.; Singh, A.; Keller, C. G.; Goldberg, K. Y.; Howe, R. T. *Proc. SPIE* **1998**, *3511*, 2.
(3) Baglio, S.; Castorina, S.; Savalli, N. *Scaling Issues and Design of MEMS*; John Wiley & Sons: Hoboken, NJ 2007.
(4) Whitney, D. E. *J. Dyn. Syst., Meas., Control* **1982**, *104*, 65.
(5) Arzt, E.; Gorb, S.; Spolenak, R. *Proc. Natl Acad. Sci. U.S.A.* **2003**, *100*, 10603.
(6) Murphy, M.; Aksak, B.; Sitti, M. *J. Adhes. Sci. Technol.* **2007**, *21*, 1281.
(7) Zhao, Y.; Tong, T.; Delzeit, L.; Kashani, A.; Meyyappan, M.; Majumdar, A. *J. Vac. Sci. Technol., B* **2006**, *24*, 331.
(8) Qu, L.; Dai, L. *Adv. Mater.* **2007**, *19*, 3844.
(9) Ge, L.; Sethi, S.; Ci, L.; Ajayan, P. M.; Dhinojwala, A. *Proc. Natl Acad. Sci. U.S.A.* **2007**, *104*, 10792.
(10) Lee, J.; Fearing, R. S.; Komvopolous, K. *Appl. Phys. Lett.* **2008**, *93*, 191910.
(11) Autumn, K.; Liang, Y. A.; Hsieh, S. T.; Zesch, W.; Chan, W.-P.; Kenny, W. T.; Fearing, R.; Full, R. J. *Nature* **2000**, *405*, 681.
(12) Mrksich, M.; Whitesides, G. M. *Annu. Rev. Biophys. Biomol. Struct.* **1996**, *25*, 55.
(13) Lieber, C. M.; Wang, Z. L. *MRS Bull.* **2007**, *32*, 99.
(14) Xia, Y.; Yang, P.; Sun, Y.; Wu, Y.; Mayers, B.; Gates, B.; Yin, Y.; Kim, F.; Yan, H. *Adv. Mater.* **2003**, *15*, 353.
(15) Ngo, L. T.; Almécija, D.; Sader, J. E.; Daly, B.; Petkov, N.; Holmes, J. D.; Erts, D.; Boland, J. J. *Nano Lett.* **2006**, *6*, 2964.
(16) Autumn, K. *MRS Bull.* **2007**, *32*, 473.
(17) Thostenson, E. T.; Li, C.; Chou, T.-W. *Compos. Sci. Technol.* **2005**, *65*, 491.
(18) Fortin, J. B.; Lu, T.-M. *Chemical Vapor Deposition Polymerization: The Growth and Properties of Parylene Thin Films*; Kluwer Academic: Norwell, MA 2004.
(19) www.torstamp.com/Brochures/BR-122.pdf.
(20) Qu, L.; Dai, L.; Stone, M.; Xia, Z.; Wang, Z. L. *Science* **2008**, *322*, 238.
(21) Chaudhury, M. K.; Weaver, T.; Hui, C. Y.; Kramer, E. J. *J. Appl. Phys.* **1996**, *80*, 30.
(22) Hertz, H. *J. Reine Angew. Math.* **1881**, *92*, 156.
(23) Johnson, K. L.; Kendall, K.; Roberts, A. D. *Proc. R. Soc. London, Ser. A.* **1971**, *324*, 301.
(24) Kustandi, T. S.; Samper, V. D.; Yi, D. K.; Ng, W. S.; Neuzil, P.; Sun, W. X. *Adv. Funct. Mater.* **2007**, *17*, 2211.
(25) Geim, A. K.; Dubonos, S. V.; Grigorieva, I. V.; Novoselov, K. S.; Zhukov, A. A.; Shapoval, S. Yu. *Nat. Mater.* **2003**, *2*, 461.
(26) www.3m.com/sg-iatd/products/pdf/structural_adhesives/3M_Scotch_Weld_Epoxy_Instant_Adhesives.pdf.

NL900343B

Hybrid core-shell nanowire forests as self-selective, chemical connectors

Hyunhyub Ko[*,†,‡,§], Jongho Lee[¶,§], Bryan E. Schubert[*,§], Yu-Lun Chueh[*,†,‡], Paul W. Leu[*,†,‡], Ronald S. Fearing[*,‖], and Ali Javey[*,†,‡,‖]

[*]Department of Electrical Engineering and Computer Sciences, University of California at Berkeley, Berkeley, CA, 94720, USA.

[†]Materials Sciences Division, Lawrence Berkeley National Laboratory, Berkeley, CA 94720, USA.

[‡]Berkeley Sensor and Actuator Center, University of California at Berkeley, Berkeley, CA, 94720, USA.

[¶]Department of Mechanical Engineering, University of California at Berkeley, Berkeley, CA, 94720, USA.

[§]These authors contributed equally.

[‖]Corresponding authors: ajavey@eecs.berkeley.edu, ronf@eecs.berkeley.edu

Supporting Information

Nanowire growth. Ge NWs with diameter, *d*=20-30 nm and length, *L*~30 μm were grown by chemical vapor deposition on Si/SiO_2 (~50 nm thermally grown) support substrates by a vapor-liquid-solid process as previously reported elsewhere[1]. Gold nanoparticles (10 nm diameter, Ted Pella) were deposited on a poly-L-lysine (0.1% w/v aqueous, Ted-Pella) modified Si/SiO_2 (50 nm, thermally grown) substrate. Ge NWs were then grown at 280 ºC and 45 torr using germane (12 sccm, 10% balanced in H_2) as the precursor gas with a typical growth rate of ~1 μm/min.

Parylene coating. Parylene-N was deposited on Ge NW arrays by using a PDS 2010 Labcoter 2 (Specialty Coating Systems) deposition system. A typical deposition condition used in this work was 160 ºC for the vaporization of the parylene dimer precursor, 650 ºC for the pyrolysis of the dimers into monomers, and 55 mTorr for the vacuum chamber. The sample was maintained at room temperature. The thickness of parylene was controlled by the amount of the loaded precursor.

Macroscopic adhesion test. The macroscopic adhesion tests were performed by first applying a normal preload force to the NW connectors (~0.5×0.6 cm^2) followed by applying a shear force, and finally removing the preload to measure the pure shear force strength.

Microscopic adhesion test. The microscopic tests used a custom two-axis force sensor[2] with a resolution of 0.4 mN at 1 kHz and range of 1.71 N. The probe was a spherical glass lens with radius of curvature of 5.17 cm. A pristine glass lens was used for the NW/glass microscale adhesion tests while a glass lens with Ge/parylene NW forests grown on the surface was utilized

for the NW/NW tests. This probe gave a contact area of 1-5 mm^2, depending on the indentation depth. First, NW forests grown on flat Si/SiO_2 substrates were fixed to a nanopositioning stage (P-611 Nanocube, Physik Instrumente. Resolution of 10 nm, range of 100 μm). Then, the stage was moved in the normal direction until the NW arrays were loaded with a prescribed force. For the case of indentation experiments, the stage was immediately retracted to disengage the NW arrays. For the shear experiments, the stage was moved in the shear direction by a specified distance, and then it was retracted in the normal direction (see Fig. S3). Indentation, shearing and retraction were all performed at 10 μm/s.

Calculation of the contact area and bending stiffness

Adhesive contact width (w) between two parallel cylindrical NWs is calculated from the following equation[3,4] based on the JKR mechanics[5],

$$P = 2\pi E^* \frac{w^2}{16R_{NW}} - \sqrt{\pi E^* w W} \quad (1)$$

where $1/E^* = 2\left(1-v_{NW}^2\right)/E_{NW}$, E_{NW} is Young's modulus, v_{NW} is Poisson's ratio, R_{NW} is the radius of a nanowire, W is work of adhesion and P is an applied normal force per unit length. For pristine Ge NWs, we assumed Hertzian contact (W = 0 in Eq. (1)). Fig. 3d shows the adhesion contact width (w) between two nanowires overlapped by 5 μm under a normal force of 200 nN with E_{ge} = 103 GPa, v_{ge} = 0.28, W_{ge} = 1200 mJ/m^2, E_{pa} = 2.8 GPa, v_{pa} = 0.4, and W_{pa} = 120 mJ/m^2. Bending stiffness, defined by an applied moment (M) over a corresponding curvature (k), is EI (= $E_{ge}I_{ge}+E_{pa}I_{pa}$) from the elastic beam theory[6], where I is an area moment of inertia.

Calculation of the contact area enhancement for interpenetrating NWs as compared to that of NWs on flat surfaces

The length over which the NWs make contact is estimated from the indentation depth data of engaged NW connectors. For simplicity, it is assumed that the NWs interpenetrate perfectly with an upper bound on the contact length between two NWs in contact being equal to the indentation depth. Indentation depth of ~26 μm is observed for the engaged NW connectors with t_p=50 nm (Fig. S2b). For NWs contacting flat surfaces, the contact length depends on the ability of the NWs to make side contact[7]. The critical length, L_{cr}, necessary to make side contact depends on the bending stiffness, EI and the energy of adhesion per unit length, ω,

$$L_{cr} = \frac{\pi}{2}\sqrt{\frac{EI}{2\omega}}$$

where,

$$\omega = 6\left[\frac{(1-\nu^2)R^2W^4}{\pi E}\right]^{1/3}$$

The NW length of 30 μm can be used as the critical length to solve for the largest radius that still allows side contact, $R_{cr}=R_{NW}+t_{p,cr}$, where R_{NW}=15 nm. The work of adhesion between glass and Ge, or glass and parylene is equal to $W_{12} = 2\sqrt{\gamma_1\gamma_2}$, where the surface energy of glass is γ_{glass}=47 mJ/m^2, Ge is γ_{glass}=600 mJ/m^2 and parylene is γ_{glass}=60 mJ/m^2. These values give a critical shell thickness of $t_{p,cr}$=184 nm. Any NW with a shell thickness above this number is not able to engage in side contact with a flat glass surface, meaning their contact area will be limited by the size of the NW tip. NWs with shell thicknesses below $t_{p,cr}$ have a contact length that is governed by the applied load per NW. If the NW is allowed to slip during the preloading until it makes side contact, it is found that the contact length is more than 70% of the NW length for loads as small as 0.1 nN per NW [7~~6~~]. However, in the case of the indentation experiments on glass, the

wires indent at most 17% of the total length with an average load of 1.2 nN per nanowire, assuming a density of 1 NW/μm^2. Therefore, it is safe to conclude that for NWs with shell thicknesses below 184 nm, all of the indented length is in side contact. In the case of t_p=50 nm, the contact length of NWs on NWs is ~5x higher than the contact length of NWs on glass. For t_p=200 nm the difference is > 25x because the stiffer NWs cannot engage in side contact on flat surfaces. This simple calculation is consistent with the experimental results (Fig. 3a).

Finite element analysis of nanowire failure

We performed failure analysis of NWs by using the finite element method to evaluate the failure modes. We used a 2D plane stress model for a 30 μm long NW with a Ge core of 30 nm and parylene shell of 50 nm. For the Ge core, we used E = 103 GPa, υ = 0.26, ρ = 5323 kg/m^3 and for the parylene shell, we used E = 2.8 MPa, υ = 0.4, ρ = 1110 kg/ m^3, σ_y = 43 MPa . One end of the NW is fixed and we studied the failure mode of the NW with increasing the interpenetration depth. For small penetration depths, the failure mode is due to interfacial failure, where the parylene shell shears off of one another. For this analysis, we assumed the interfacial shear stress is 2 MPa[8], though this particular value may vary depending on surface roughness and the surface functionalization. For larger penetration depths (> about 3 μm), the NWs are sufficiently attached to one another, and thus the failure mode is due to local yielding of the parylene, resulting in necking of the parylene, and breaking of the Ge core. The parylene begins to yield at a force of about 720 nN of axial force.

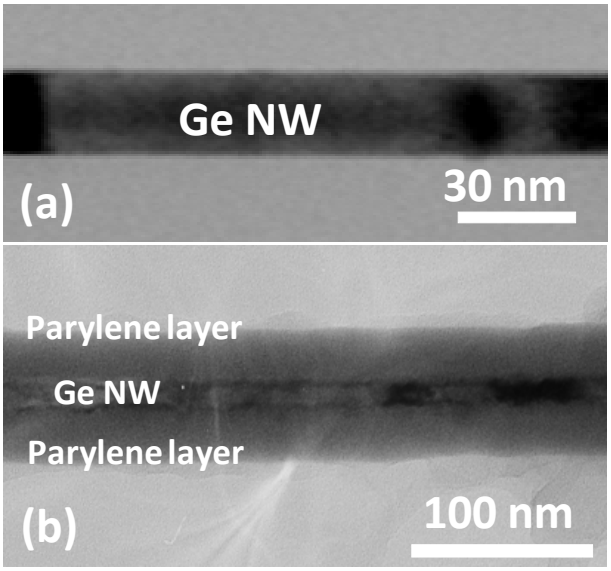

Figure S1. Representative TEM images for (a) a pristine Ge NW and (b) a Ge/parylene core/shell NW, depicting the magnitude of the NW surface roughness.

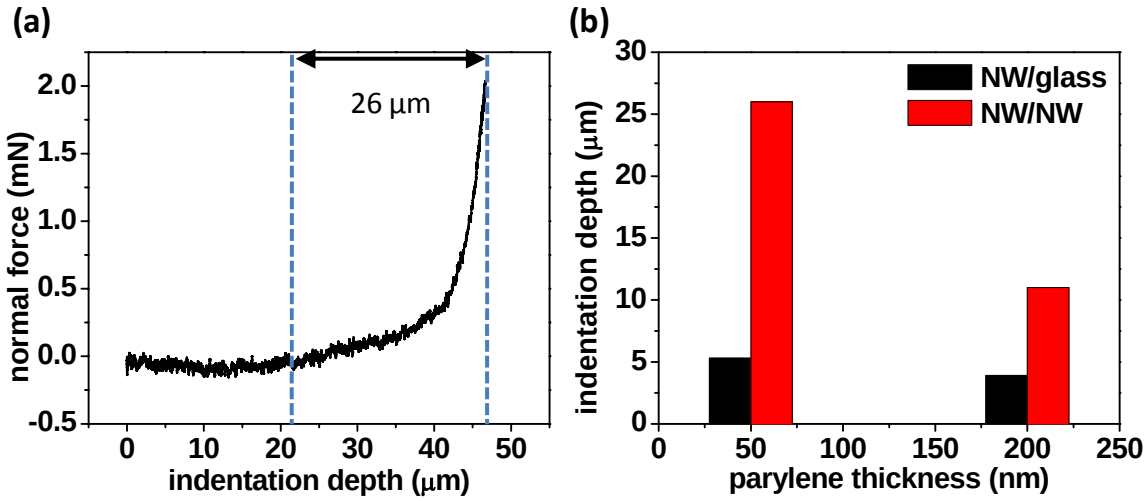

Figure S2. (a) Microscale NW/NW indentation tests for t_p=50 nm, indicating ~26 μm maximum indentation depth with a 2 mN preload force. (b) Indentation depths for NW/NW and NW/glass at 2 mN preload for different parylene thicknesses (50, 200 nm).

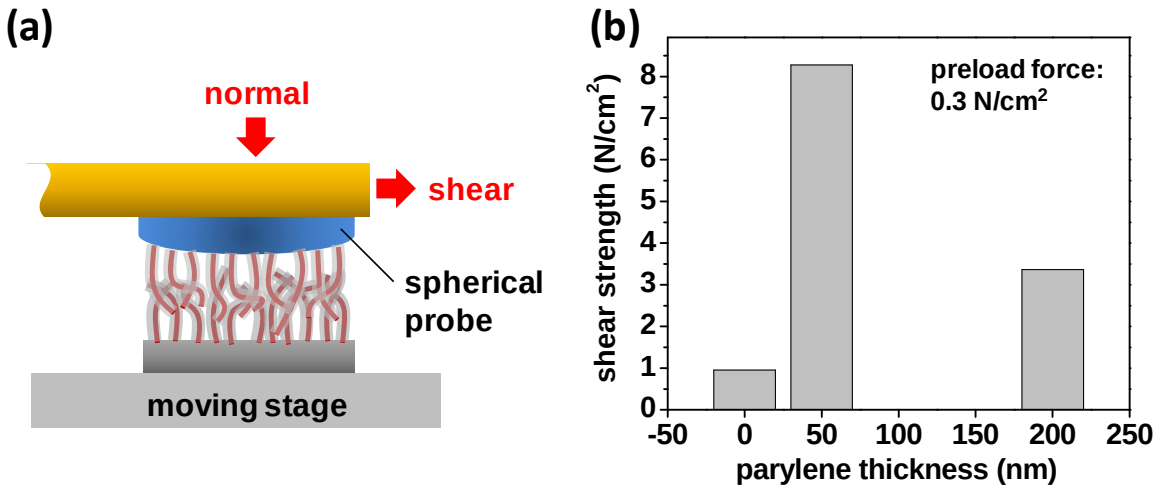

Figure S3. NW connector characterization using the microscale force sensor. (a) Schematic of the microscale adhesion tests, showing a spherical probe (radius of curvature of 5.17 cm) coated with the hybrid NW forest on the surface. For the measurements, the probe is brought in contact with another NW forest grown on a planar substrate followed by the application of normal, followed by shear forces. (b) Maximum shear force measured for 0.3 N/cm^2 normal preload force sheared until failure as a function of parylene shell thickness.

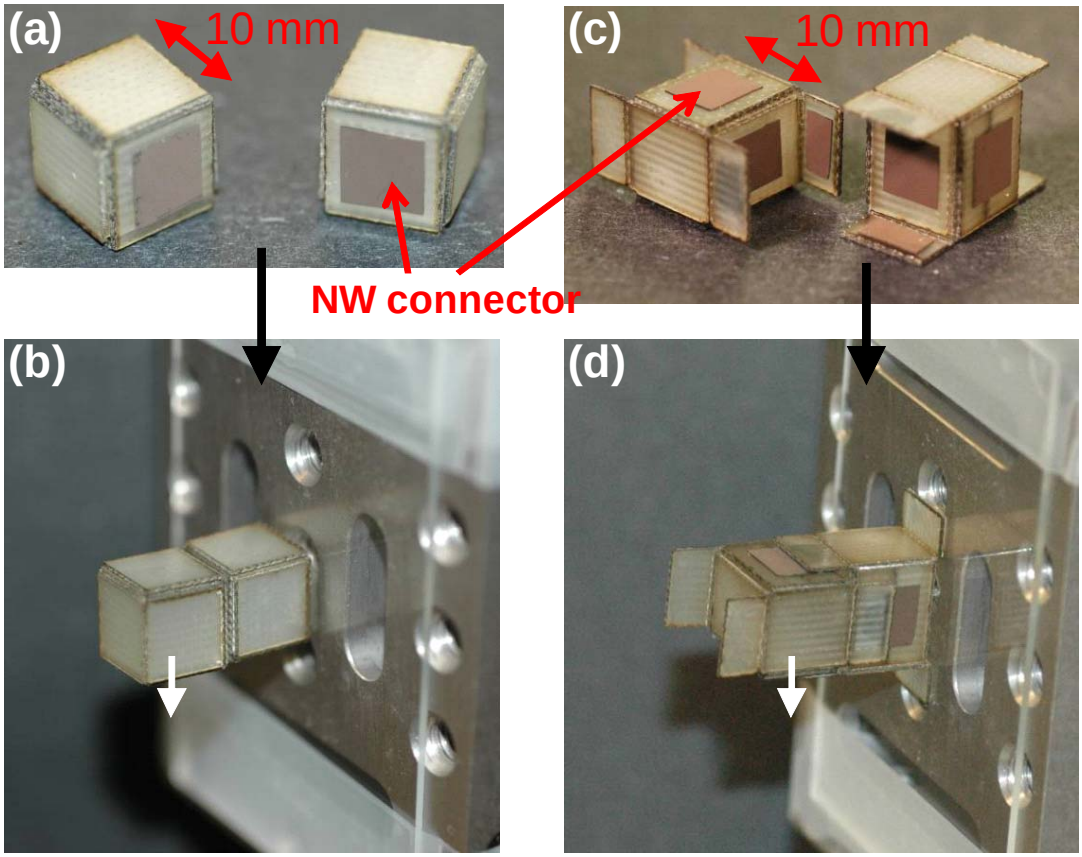

Figure S4. 50 nm parylene-coated NW connectors holding together cubes into a cantilever configuration. (a,b) Simple cube with connectors on cube face. (c,d) Tabbed cubes with connectors on cube faces and tabs to provide higher resistance to moments. White arrow shows loading position (center of outer cube). The cubes are made of 10 mil thick glass fiber composite with 1 mil thick polyester flexure layer. The simple cubes and tabbed cubes can be connected through nanowire connectors by applying slight hand-pressure. This cantilever shape can be taken apart and put back together reversibly for potential use in reconfigurable structures.

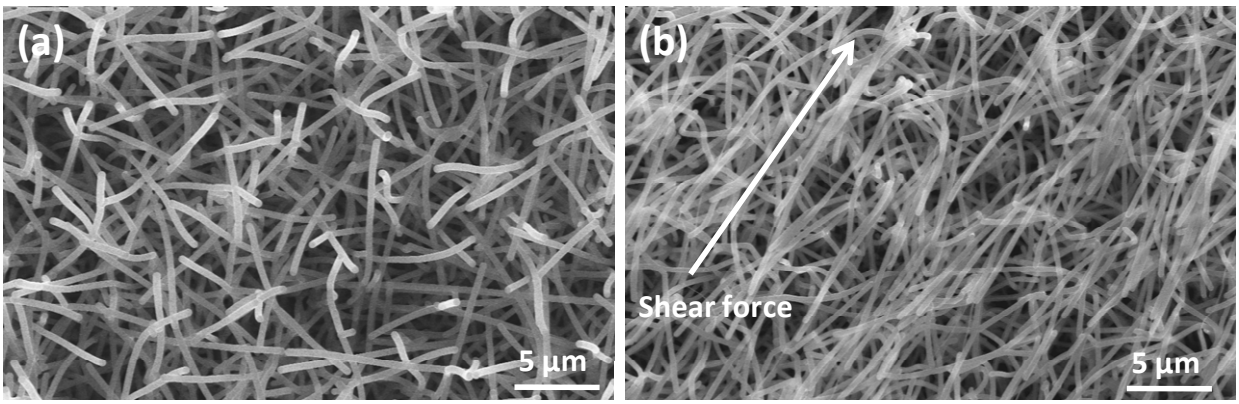

Figure S5. SEM images of hybrid NW forests (a) before and (b) after shear adhesion test, showing the shear-induced NW alignment in the direction of the applied shear force. This alignment enhances the contact area between the interpenetrating NWs in the shear mode, resulting in high shear adhesion strength.

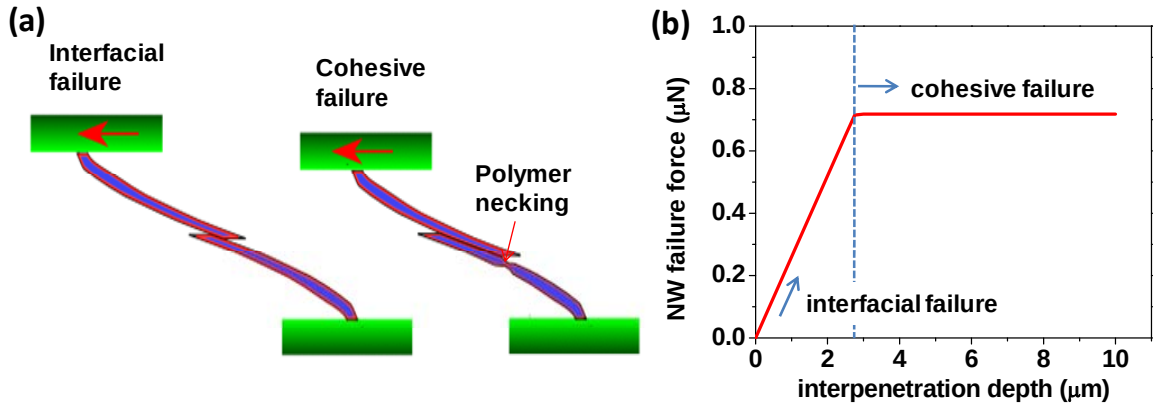

Figure S6. The modeled shear strength for 2 NWs contacted in parallel as a function of the contact length (i.e., interpenetration depth). For low indentation depths, interfacial failure (i.e., breakage of vdW bonding) is the dominant failure mechanism. For large indentation depths, cohesive failure, such as Ge core breakage and polymer necking, is the main cause of adhesion failure.

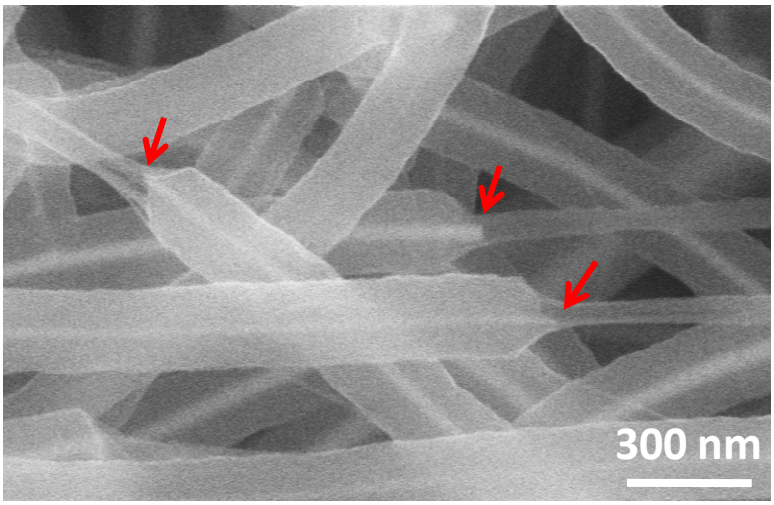

Figure S7. SEM image of a hybrid NW forest after shear failure. Red arrows indicate the polymer necking and rupture, resulting in cohesive failure.

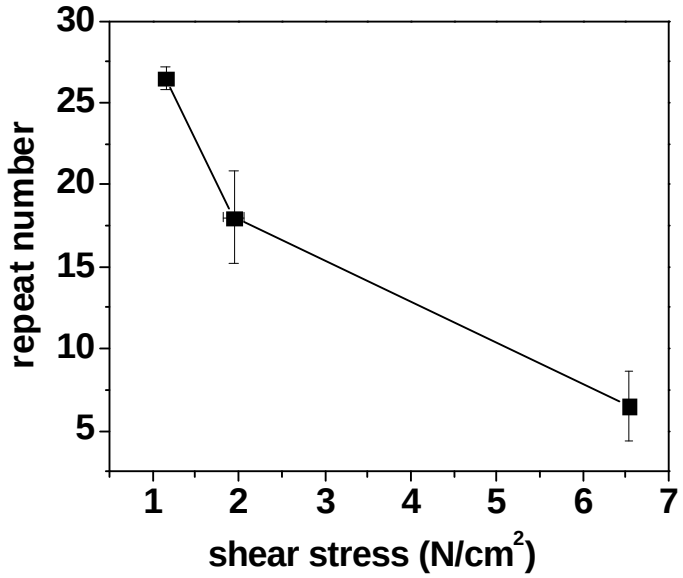

Figure S8. Reusability test of hybrid NW connectors with t_p=200 nm with an applied preload force of 0.8 N/cm^2. Repeat numbers represent the number of subsequent loading and unloading cycles a sample could withstand when subjected to a specific shear stress. Since the surface morphology of NW connectors change after repeated use as can be seen in Fig. S5, the binding properties also change after multiple cycles of operations. For example, NW connectors with t_p=200 nm showed ~44% decrease in the shear adhesion strength and ~15% increase in the shear to normal ratio after 5 operation cycles (with preload of 0.8 N/cm^2 and shear load of 1.2 N/cm^2).

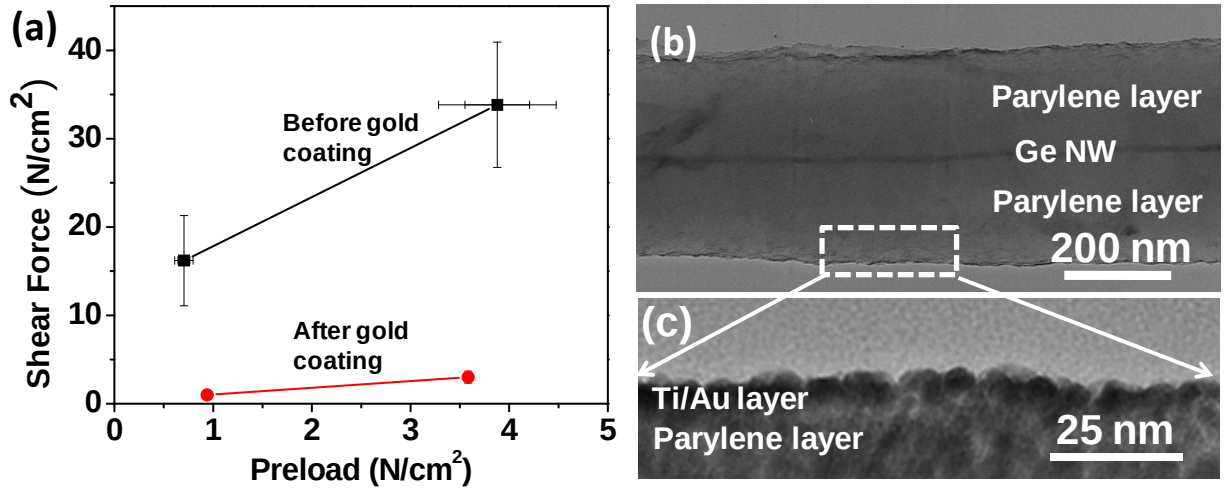

Figure S9. (a) Shear adhesion force of NW connectors with 200 nm parylene thickness before and after gold coating (Ti/Au, 2/3 nm, deposited by electron-beam evaporation). (b) and (c) TEM images of a Ti/Au coated hybrid NW, showing the enhanced surface roughness after metal deposition. The ultrathin gold coating hardens the surface, without significantly affecting the overall NW stiffness. The drastic reduction in the shear force by the application of an ultrathin layer Au depicts the dominant role of vdW interactions (as opposed to mechanical entanglement) in the NW connectors, for which intimate contact enabled by soft surfaces is essential. The conformal contact is reduced for rough and hard Ti/Au coated surfaces.

References

[1] Fan, Z.; Ho, J. C.; Jacobson, Z. A.; Yerushalmi, R.; Alley, R. L.; Razavi, H.; Javey, A. *Nano Lett.* **2008**, *8*, 20.

[2] Schubert, B.; Majidi, C.; Groff, R. E.; Baek, S.; Bush, B.; Maboudian, R.; Fearing, R. S. *J. Adhesion Sci. Technol.* **2007**, *21*, 1297.

[3] Chaudhury, M. K.; Weaver, T.; Hui, C. Y.; Kramer, E. J. *J. Appl. Phys.* **1996**, *80*, 30.

[4] Hui, C. Y.; Lin, Y. Y.; Baney, J. M.; Jagota, A. *J. Adhesion Sci. Technol.* **2000**, *14*, 1297.

[5] Johnson, K. L.; Kendall, K.; Roberts, A. D. *Proc. R. Soc. London. A.* **1971**, *324*, 301.

[6] Crandall, S. H.; Dahl, N. C.; Lardner, T. J. An introduction to the mechanics of solids; McGraw-Hill: New York, **1978**.

[7] Majidi, C. S.; Groff, R. E.; Fearing, R. S. *J. Appl. Phys.* **2005***, 98*, 103521.

[8] Fortin, J. B.; Lu, T.-M. Chemical Vapor Deposition Polymerization: The Growth and Properties of Parylene Thin Films; Kluwer Academic: Norwell, MA **2004**.